2022

Characterizing Bacillus subtilis colony morphology in response to environmental acidification

BOSTON UNIVERSITY

GRADUATE SCHOOL OF ARTS AND SCIENCES

Thesis

CHARACTERIZING *BACILLUS SUBTILIS* COLONY MORPHOLOGY IN RESPONSE TO ENVIRONMENTAL ACIDIFICATION

by

ALYSSA B. HAYNES

B.A., Boston University, 2022

Submitted in partial fulfillment of the

Requirements for the degree of

Master of Science

2022

Approved by

First Reader

Joseph Larkin, Ph.D.
Assistant Professor of Biology and Physics

Second Reader

Sarah Davies, Ph.D.
Assistant Professor of Biology

Third Reader

Jeffrey Marlow, Ph.D.
Assistant Professor of Biology

DEDICATIONS

This thesis is dedicated to my parents and siblings whose constant support made this work possible. They are role models, mentors, and friends who I am lucky to know and love. This thesis is also presented in the loving memory of my grandmother.

CHARACTERIZING *BACILLUS SUBTILIS* COLONY MORPHOLOGY IN RESPONSE TO ENVIRONMENTAL ACIDIFICATION

ALYSSA B. HAYNES

ABSTRACT

Bacterial community dynamics in the human gut microbiome can have profound effects on human health and disease, yet experimental limitations make it extremely difficult to study this environment with sufficient ecological validity. To work toward physiological relevance, this study ostensibly aimed to assess the morphological changes in *Bacillus subtilis* colonies in response to pH transience. However, before observing colony responses at pH transition points, static hard substrate experiments in acidic conditions revealed a novel colony growth phenotype. The bulk of the work that follows this observation aims to characterize and explain the novel 'microcolony' phenotype; this phenotype is characterized by an asymmetrical formation of cell clusters within the inoculation drop initially, which then converge to form a dense, cohesive colony with minimal radial expansion. Experiments revealed a lack of swarming motility and increased chaining in acidic conditions – with no evidence to support a pH sensation and chemotaxis element to the phenotype. Our results suggest that apparent increased cell-cell adhesion under acidic conditions is a result of both pH-driven matrix protein aggregation and a pH-driven defect in cell division machinery. While both theories are strongly supported by our findings and the existing literature, we recommend further experiments to assess the contributions of each of these factors in determining colony morphology.

TABLE OF CONTENTS

INTRODUCTION

Characterizing the human gut microbiome

Humans and ruminant animals serve as hosts for numerous microbial species dispersed throughout the distinct microbiomes in and on the body. The skin, oral, respiratory, vaginal, and gut microbiomes in humans have drastically different environments and community compositions, yet all have been found to impact human health and disease. Often viewed as the most prominent of these microbiomes, the human gut microbiome is highly complex with spatiotemporal heterogeneities in both environmental conditions and microbial composition. The gut microbiome consists of bacteria, eukaryotic organisms, viruses, and their genes and metabolites in close association with the mucosal lining of the host epithelium. The microbes in the human gut develop into a complex of 10-100 trillion symbiotic cells that assist in host functions such as digestion and epithelial tissue renewal [54].

While it is the topic of many investigations, the origins of the gut microbiome remain highly mysterious. The development of an individual's gut microbiome begins at birth and, as such, can depend on the mother's skin and vaginal microbiome compositions as well as the mode of delivery [55]. This microbiome continues to adapt to the changing intestinal environment during the child's development and corresponding dietary shifts [9]. Studies also indicate that the host evolutionary history and diet in adulthood influence the community composition within individuals [33]. Repeated use of antibiotics, probiotics, NSAID medications, and antacids has been shown to have significant effects on the gut

microbiome composition [43, 6, 37, 8]. In addition, host tissues secrete both specific and nonspecific factors to selectively promote the growth of some microbes over others with the goal of maintaining host health [23]. In healthy individuals, the gut microbiome consists primarily of microbes from the phyla Firmicutes and Bacteriodetes [44].

Studying the human gut microbiome comes with many challenges. Until recently, hundreds of gut microbes were not able to be cultured *in vitro*, hindering laboratory studies of relevant species coculture [31]. Modern culture methods have allowed for the laboratory study of many of these microbes, but few systems involve the coculture of host epithelium to account for host-microbe interactions. *In vivo* mouse models allow researchers to observe some of these host-microbe interactions in relatively controllable organisms. Lastly, high throughput metagenomics studies can assess, given patient stool samples, trends in gut microbiome compositions among healthy individuals as compared to individuals with gut-related health issues. However, these studies are largely used to characterize rather than experiment with the microbiome. Ultimately, the human gut microbiome is one of the most difficult biological systems to study, and a combination of metagenomics, mouse models, and *in vitro* experiments is necessary to achieve sufficient ecological validity.

While difficult to study, the gut microbiome is extraordinarily significant to human interests. Human gut microbiome dysbiosis has been found to contribute to many health conditions, including but not limited to: autism spectrum disorder, chronic kidney disease, nonalcoholic fatty liver disease, liver cirrhosis, cardiovascular disease, alcohol

dependence, and Alzheimer's Disease [29, 27, 47, 49, 41, 32, 34]. While research into the mechanisms of host-microbe interactions and their influence on human health is frequently studied, emerging research also suggests a possibility for disease treatment via the targeting and regulation of the gut microbiome [59, 28]. The ability to study the human gut microbiome with sufficient ecological validity is a critical first step toward harnessing microbial interactions to promote human health.

Characterizing types of bacterial communities

As single-celled organisms, bacteria can survive and persist in a few forms that are thought to confer unique advantages to an individual cell. When a bacterium is free-living and unattached to other members of a bacterial community, this is considered the planktonic form. However, bacteria are rarely found in their planktonic form in nature due to the survival advantages of associating with other bacterial cells [24]. One form of bacterial community structure is a swarm; these communities are characterized by high motility that allows for rapid radial expansion with minimal upward growth and are thought to precede biofilm formation in natural environments [22]. Bacteria of many species can also form well-characterized communities known as biofilms.

Biofilms are communities of microorganisms encased in an extracellular matrix composed of proteins, polysaccharides, surfactants, extracellular DNA, and communal nutrients. Biofilms are found in the human GI tract, in marine environments, and alongside plant root structures in soil environments. The ability of biofilms to conduct group behaviors, share nutrients, and take on a robust physical structure attributes to the survival

advantages of existing in this form. Biofilms are significantly more resistant to antibiotics than planktonic bacteria, participate in symbiotic exchanges with nearby organisms, and defend participating cells from toxins secreted by competing microbial communities [13, 4, 45]. In the context of the human gut, biofilm formation can be the difference between health and disease states. For example, *Helicobacter pylori* causes infection by forming biofilms on the mucosal lining of the highly acidic stomach, this infection often becoming resistant to antibiotics and leading to gastric ulcers [61]. In addition, *Bacteroides fragilis* biofilms have been reported to increase in inflammatory bowel disorder patients and have been associated with an increased risk of developing colorectal cancer [60]. Thus, understanding the colony-scale structures within the human gut microbiome can be important in attempting to understand the difference between health and disease states.

Many biofilm group behaviors and survival advantages are attributed to the presence and composition of the extracellular matrix. In *Bacillus subtilis* – the model organism used in this study – biofilms, the extracellular matrix is composed of macromolecules including proteins, polysaccharides, and nucleic acids. Under regulation by SinR, the protein TasA and polysaccharide exopolymeric substances (EPS) constitute a significant portion of the biofilm matrix and have been shown to play vital roles in determining biofilm structure [7]. TasA is a soluble monomeric protein that forms β-sheet-rich fibrils in the matrix of *B. subtilis* biofilms [15]. As a functional protein, it serves to stabilize the physical structure of the biofilm and promote cell-cell and cell-surface adhesion, yet the three-dimensional structures of the proteins can be altered in response to

environmental conditions [18]. EPS, on the other hand, describes a diverse array of macromolecules that can be divided into subcategories based on the function(s) they take on in the matrix. The four major categories of EPS are as follows: structural (neutral), sorptive (charged), surface-active (ie: surfactin) and active (ie: secreted enzymes) [36].

Current work

While advances have been made in methodology, the complexity of the human gut microbiome continues to complicate *in vitro* experiments. One of the greatest challenges in studying and replicating the microbiome *in vitro* is the extensive environmental spatial heterogeneity within the human gastrointestinal tract (GIT). In addition to the microbes that colonize the lumen of the GIT, food-borne bacteria can be integrated into the transient microbiome and can have significant influence on the resident community structure and function [62, 25]. This transient microbiome can increase production of short-chain fatty acids in the gut, protect the host from opportunistic pathogens, and, in some cases, transient cells maintain metabolic activity through the GIT before arriving at the colon [14]. Therefore, rather than observing colony morphologies in static conditions that may resemble one portion of the GIT or another, we aim to develop a dynamic method of study that allows us to simulate physiological transition points. The ability to study the dynamic interactions between microbes and their environment is valuable in formulating a more complete understanding of bacterial colony growth and survival under the diverse conditions in the human GI tract.

While the transient gut microbiota experiences a variety of environmental changes throughout the GIT [35], this study will focus primarily on the drastic pH differences between GIT compartments. Over the course of approximately 24 hours on average, transient bacteria may experience pH changes that equate to a near 10^5-fold change in H^+ ion concentration [39]. From the highly acidic stomach environment (pH of 1.4 to 2), transient microbiota transition to the small intestine with pHs ranging from 6 to 7.4, then to the slightly acidic caecum (pH of 5.7), then finally the near-neutral rectum before being excreted [16]. Since the metabolic activity of transient microbes can have profound effects on the resident microbiome, and the microbes that make up this transient sub-population experience drastic transitions in environmental pH between compartments, we have the goal of investigating the macro-scale colony responses at these transition points. We chose to observe colony-scale responses because the internal pH maintenance strategies employed by bacteria under acid stress are already well characterized [20], yet little literature exists which characterizes the colony-scale responses to acidic conditions in neutrophilic bacteria.

In this study, we will be working with NCIB 3610 *B. subtilis* of the phylum Firmicutes. *B. subtilis* is a neutrophilic, gram-positive species that has a strong internal buffering capacity under a wide range of external pH values [30]. Although *B. subtilis* is generally considered a soil organism, its ability to survive metabolic stress via sporulation allows for its presence in the human gut microbiome [52]. In fact, its lack of pathogenicity, paired with this ability of *B. subtilis* to form spores and survive harsh pH conditions, makes it a suitable target organism for the development of modern probiotics [12]. Its ease of

culture, presence in some probiotics, preference for a neutral environment, and use as a model organism make it a suitable bacterial species for this study.

Before we could establish a dynamic experimental system to observe colony responses to environmental transitions, we had to develop the foundational tools to be used in those experiments. This included the development of a novel defined minimal media that can be buffered to a precise value within the physiologically relevant range of pH as well as the integration of microfluidics laboratory equipment. The static experiments during the development of these tools led to the identification of a novel growth morphology on acidic agar, the characterization of which has come to represent the bulk of the thesis work presented in this report.

MATERIALS & METHODS

Strains used

In addition to *B. subtilis* 3610 with a point mutation conferring inducibility, two mutant strains were cloned for experimentation. We attempted to delete the following genes with the reciprocal insertion of Erythromycin and Lincomycin (MLS) resistances: mcpA, tlpA, and mcpA/tlpA. McpA and tlpA have been identified as chemoreceptors responsible for sensing and chemotaxis in response to acidic environmental pH [53]. As such, their deletions were designed to investigate the influence of pH sensation and chemotaxis in the development of colony morphology on acidic substrates. Sequence identification for primer design was conducted using SubtiWiki, an online *B. subtilis* database [40]. While the ΔmcpA and ΔmcpA/tlpA knockouts were successfully transformed, the ΔtlpA knockout strain was unable to be created in time to observe its growth. In addition, occasional experiments were conducted with a dual-reporter strain of *B. subtilis* 3610 that reports on $P_{hag} - YFP$ (motility genes) and $P_{TapA} - mCherry$ (matrix production genes).

Culture growth assays

Colony growth was quantified using one of two strategies: plate reader analysis of liquid culture and colony forming unit (CFU) measurement. The BioTek Synergy H1 plate reader was used primarily for media development and assessment of overall *B. subtilis* growth under various liquid culture conditions. While these measurements offer valuable information about relative growth, the readout is an optical density (OD) measurement

which cannot be directly interpreted as a viable cell count. Conversely, when quantifying colony growth on hard substrates – such as agar plates – CFU counts were conducted by scraping the colony off its substrate and resuspending in 1x PBS. CFU counts must be conducted when cells are not cultured in liquid media, but in scraping the cells off the agar pads, some cells will be left behind, introducing an inherent source of error. This method, however, does give a direct readout of viable cell density and is effective in comparing growth and viability of colonies under different conditions.

Creation of an ideal growth medium

Msgg is a commonly used defined minimal media for culture of *B. subtilis*. With its rigid, neutral MOPS buffer system and biofilm-promoting capabilities [50], it is an ideal media for many experimental designs. However, the need to tightly control the pH of the growth media along a range of pH values in this study facilitated the development of a novel medium. The nutrient and ion concentrations in this medium must change minimally when titrated to low pH values to limit unintended effects on cell growth. Importantly, carboxylic acids – such as those found in citric acid – can efficiently chelate metals in solution [46], rendering them unavailable for use by the cells in culture. Thus, the ideal media would have a flexible buffer system, sufficient nutrients to support Msgg-like growth, and a source of acidity that does not involve carboxylic acid functional groups. M9 minimal media was a promising candidate because of its similarity of salt composition to Msgg and its sodium/potassium phosphate buffer system that can be altered to produce acidic, neutral, and basic variations. Initial trials involved liquid culture growth assays to

determine the extent of growth that could be supported by M9 using a recipe from Cold Spring Harbor protocols [11].

Liquid culture growth assays using the Biotek plate reader revealed a growth discrepancy between Msgg and neutral M9. To mitigate this difference, several conditions were tested in which elements of M9 and Msgg were exchanged to preserve the ideal buffer system of M9 while supporting Msgg-like growth (Figure 1a). The condition that most closely resembled growth in Msgg was the following: M9 with the removal of glucose as a carbon source, replacement with glycerol and glutamate at the concentrations found in Msgg, and addition of iron and manganese at the concentrations found in Msgg. This modified M9 medium (MM9) serves as the ideal medium for acidic growth assays in this study. Once MM9 was formulated, cells were cultured in acidic MM9 (pH ~5.25) to ensure that this variation also supported significant cell growth in liquid culture (Figure 1b). While some MM9 nutrient concentrations vary from those in Msgg (Table 1), growth and colony formation in MM9 was deemed sufficient for experimentation.

Colony culture on agar substrates

Agar substrates were created by mixing the desired media (Msgg, neutral MM9, or acidic MM9) with agar powder. Once cooled, the agar hardens and creates a semi-solid surface for colony culture. Agar concentration significantly affects the type of colony that forms; typically for biofilm culture, 1.5% agar is used, whereas 0.5% agar is used to induce swarm formation. In all comparative experiments, all types of agar are left to harden and desiccate for the same amount of time after pouring equal volumes into a multi-well plate.

Colony culture begins with an LB streak plate of the frozen stock for the strain of interest. Once colonies form after overnight incubation at 37˚C, one colony is scraped using a pipette tip and resuspended in 250 µL of 1x Spizizen Salts [51]. 100 µL of this solution is then plated on a premade Spizizen Salt-based minimal media plate with a glucose carbon source and 1.5% agar. The plate is shaken with plating beads to distribute the cell mixture uniformly over the surface of the agar, then left to grow overnight at room temperature or for 6 hours at 37˚C. Once a light lawn has formed, the cells are rinsed from the plate using a neutral minimal medium (such as M9), and this mixture is left in the 37˚C shaking incubator for approximately 3 hours, or until the culture has reached 0.4 OD. The cells are then spun down and washed two times with the media that corresponds with the agar plate to be used. 1.5 µL of this mixture is then placed in the center of the plate and can be imaged once the inoculation drop has dried.

Colony culture in a microfluidics system

The Millipore Sigma CellASIC ONIX2 Microfluidics System was used for all microfluidics data collected. This system uses optically clear prefabricated plates (B04F) with four chambers that each have two cell traps for initial colony establishment. The system allows for constant nutrient replenishment with laminar flow of the growth media. With the use of its included software, we can precisely control and program pressure, gas, and temperature settings over the course of an experiment. In our experiments, cell culture was loaded at a high density (OD 1.0+) to trap small clusters of cells in the chamber, and the flow was set to 1.26 psi during growth and imaging.

Microscopy, image analysis, and data visualization

The BioTek Lionheart FX inverted imager was used for all fluorescence and time lapse microscopy in this study, including time-lapse microscopy of the microfluidics system described above. This automated benchtop microscope – equipped with Gen5 Microplate Reader and Imager Software – is capable of incubating and imaging a multi-well plate, allowing for a high level of control when comparing colony phenotypes during growth in multiple conditions. In addition, an iPhone 13 or Nikon D7500 DSLR camera was used for high-resolution still images of whole colonies without fluorescence. Once collected, images were analyzed, and quantitative measurements were extracted using ImageJ software [48]. Figures were created using IPython (Jupyter) Notebook. In data visualization, care was taken to consider color vision deficiency, and all figures were checked using Coblis, a color blindness simulator [10].

RESULTS

Identification of a novel growth phenotype on acidic MM9

After the novel MM9 medium was developed, it was important that it was tested in the context of hard substrate (1.5% agar) biofilm culture to ensure that it supports growth and colony formation comparable to commonly used media like Msgg. In the neutral condition, colonies appeared large and cohesive after 48 hours of growth with a border morphology resembling that of a colony grown on Msgg. Thus, the neutral form of the media was deemed sufficient to support biofilm establishment. On the acidic version of MM9, however, we discovered a novel 'microcolony' growth phenotype (Figure 2). In an experiment using Thioflavin T (ThT) to stain the cell membrane, we identified clusters of cells in the acidic version of MM9 that grow independently of one another. These microcolonies can have different growth rates from one another and at around 48 hours of growth begin to converge. After this joining, the colony typically takes on an irregular shape but continues to grow as one colony. Throughout growth on acidic MM9 agar, the colonies have sharply defined borders and minimal radial expansion. Despite the reduced colony expansion, the acidic media does, in fact, support the growth of colonies on agar substrates.

To ensure that this microcolony phenotype was not simply an artifact of dispersed surviving cells with spontaneous acid resistance, we assessed the growth differential between neutral and acidic colonies. First, cells from the same preculture mixture were plated on replicates of 1.5% agar made of both neutral and acidic MM9. Throughout the

96.75 hours of growth, eight CFU counts were conducted for both acidic and neutral colonies, and the results were plotted. The resulting graph displays the approximate tenfold increase in viable cells from acidic to neutral colonies, but the acidic condition still supported a normal growth curve, with no evidence of a major die-off event (Figure 3). This finding inspired the next experiment in which the inoculation culture was gradually diluted and serially plated on neutral MM9 agar. We hypothesized that if the microcolony phenotype was solely a result of the growth differential between neutral and acidic conditions, then the resulting colony in the (10:1) diluted neutral MM9 condition would also take on this 'microcolony' form. However, there are several key differences between the growth phenotypes of the diluted inoculation on neutral MM9 and the standard inoculation on acidic MM9. While initial growth is dispersed across the diluted inoculation spot, the mature colonies (48+ hours of growth) have the same edge morphologies across all tested dilution magnitudes. Thus, the different growth morphologies on acidic and neutral substrates are a result of more complex molecular dynamics than simply differential survival and growth rates.

Conditions for maintenance of microcolony phenotype

Before continuing to explain the microcolony phenotype, we decided to characterize the lowest pH value that supports significant growth in culture and compare the growth in liquid culture to hard substrate experiments. First, we experimented with a microtiter plate in which each row had cells growing in liquid MM9 at a pH within the range of 4.24-7.01. The exponential growth phase was very similar in slope for all

conditions that successfully grew, suggesting a similar growth rate in liquid media ranging from pH 7.01 to 4.84 (Figure 4a). The cultures in media of pH 4.84 grew at a similar growth rate as neutral, yet they do not continue growth to the same final cell density as the higher pH conditions. While the exponential phase initiation time varied slightly between conditions, this slight difference does not appear to correlate clearly with media pH. There was virtually no growth at a pH of 4.24, suggesting that the growth threshold for *B. subtilis* in liquid MM9 lies somewhere between a pH of 4.84 and 4.24.

We then assessed the growth threshold for B. subtilis on 1.5% agar of varying levels of acidity. Due to the nature of agar, pH strips were used in lieu of a pH meter in determining the pH of the agar. Thus, precise pH measurements were not possible, so the experimental values are approximated to the nearest integer. Three days post-inoculation, colonies successfully grew on all five agar conditions ranging from a pH of 8 to 4 (Figure 4b). This is evidence of a difference in the lower bound pH threshold required for growth in *B. subtilis*. It should be noted that agar below pH 4 will not solidify at room temperature, and thus cannot be inoculated, making it difficult to provide a conclusive statement of the value of the lower bound pH growth threshold on hard substrates.

Probing the influence of motility and chemotaxis on the microcolony phenotype

Since all experiments up to this point had probed the differences between biofilm morphologies on acidic and neutral agar, we decided to also assess how swarming morphologies varied between the two conditions. Experimentally, swarming can be induced in *B. subtilis* by using a less structured, softer agar substrate. In our experiment,

we altered agar substrate hardness along a gradient from 0.5% to 2.0% using Msgg, neutral MM9, and acidic MM9. While colony expansion appeared to inversely correlate to agar percentage – in line with our expectations – for both neutral conditions, the acidic colonies maintained a similar lack of radial expansion even at low agar concentrations (Figure 5). When colony surface area after 48 hours of growth is plotted, the acidic colonies do not follow the same growth expansion patterns as the neutral colonies, suggesting an inhibition of the swarming phenotype by a low-pH environment (Figure 6). While the agar hardness may also be affected by the pH of the media, as noted above, this should, in theory, enhance the radial expansion of a colony grown on the softer acidic agar rather than suppress expansion. This is further evidence that the three-dimensional colony structure on acidic MM9 agar significantly inhibits colony radial expansion, perhaps by increasing cell-to-cell adhesion.

To test the hypothesis that the colony morphologies differ because of a pH sensing and response mechanism, we created the following knockout strains: ΔmcpA and ΔmcpA/tlpA (see Methods). According to the assumption that these genes are responsible for pH sensation and chemotaxis, if the phenotype is related to chemotaxis, then knockouts on both acidic and neutral MM9 should look similar to one another, and we will not see the microcolony phenotype. However, when plating the mutant strains on acidic agar, we see evidence of microcolony formation in early growth and minimal radial expansion overall, in line with the morphologies of WT (Figure 7). Like WT colonies, the mutant strains were unable to swarm at lower agar concentrations. Thus, from our experiments, it does not seem likely that the microcolony and later growth phenotypes on acidic MM9

agar are formed because of pH-driven chemotaxis. Given more time for data collection, we would have liked to run a microfluidics experiment with the mutant strains to assess the smaller-scale dynamics in these colonies in an acidic environment, as compared to WT.

Observing colonies under greater magnification

To observe the ways in which colonies navigate transitions in environmental pH over time, we employed a microfluidics system. In this experiment, we loaded cells into the microfluidics device at a very high density and thus had cell clusters stuck beside the traps as well as underneath them. After 12 hours of neutral MM9 media flow, the experimental chamber (B) switched to acidic MM9, while the control chamber (A) remained neutral. We used the hag/TapA dual-reporter strain (see Methods) in this experiment, but the exposure time was not high enough to capture the mCherry channel in any of the chambers, rendering matrix and motility data unavailable. Nearly immediately after the transition to acidic MM9, cells in chamber B started chaining heavily while pre-existing dense colonies largely dissipated (Figure 8). Meanwhile, the neutral control chamber saw some chaining only on the edges of established colonies as they grew and became denser. Thus, this experiment allowed us to visualize a cell division defect in response to acidic MM9 that we were not able to visualize through the agar substrate. Since this change happened so quickly after the transition to an acidic environment, it is likely that the cell division defect is due to altered ionic states of enzymes and substrates rather than altered gene expression.

To determine whether this chaining phenotype is influenced by the flow conditions in the microfluidics device, we conducted an inverted agar experiment. The inverted agar experimental setup enables high-magnification imaging of growing cells with vertical growth constrictions. This is done by inoculating a small square of agar with the cell culture mixture, allowing that spot to dry, then flipping over the agar onto a glass-bottom plate. The inverted imager can now focus on cells at 40x magnification since it does not need to image through millimeters of agar. Although the colonies were not restricted to single-layer growth for the entirety of the experiment, we were able to observe growth at single-cell magnification on acidic MM9 agar without flow. There was significant chaining when cells were grown on inverted acidic MM9 agar, suggesting the flow conditions did not create this chaining phenotype (Figure 9). This is evidence that the microcolony phenotype on agar substrates may be related to a cell division defect that results in increased cell chaining.

DISCUSSION

This study, although deviating from the original experimental design aimed at observing physiological pH transitions, revealed a significant amount about *B. subtilis* responses to an acidic environment at the colony level. On hard substrates, acidic colonies grow in an asymmetrical, patchy pattern termed the 'microcolony' phenotype until they merge to form a thick, cohesive biofilm with little radial expansion. The complete proposed explanation for the microcolony phenotype is summarized in Figure 10 and is detailed in the following discussion.

Matrix aggregation theory

Initially viewed as the primary force driving the unique growth of colonies in acidic conditions, the matrix aggregation theory hinges on the biochemical principle of isoelectric point and its involvement in protein aggregation. The isoelectric point of a protein/macromolecule is the pH value (± 1) at which the net charge of its amino acid residues equals zero. When the peptide loses its charge around its isoelectric point, it becomes more hydrophobic and is more likely to aggregate with other uncharged macromolecules due to the hydrophobic effect. Our theory is that the acidic pH of the growth medium is near the isoelectric point of the macromolecules in the biofilm matrix, causing macromolecule aggregation, and increasing cell-to-cell adhesion in turn. Although the biofilm matrix is highly complex, we have identified TasA and exopolymeric substances (EPS) as the most likely macromolecules responsible for the phenotypic

expression of the theory due to their physical properties and prevalence in the matrix of *B. subtilis* biofilms.

According to SubtiWiki, the major *B. subtilis* biofilm matrix protein, TasA, has an isoelectric point of pH 5.44. This value is strikingly close to the pH of acidic MM9, suggesting that TasA is likely neutrally charged in our acidic experimental conditions. Dual reporter strain (see Methods) experiments suggested the production of TasA under both neutral and acidic conditions, but we were unable to characterize the three-dimensional structure of the protein in living biofilms without the necessary laboratory tools. However, existing *in vitro* studies of purified TasA show the propensity of the protein to aggregate in solution around the theoretical isoelectric point, which they calculate to be approximately pH 5.2. In this study, the authors determine that the low-pH-induced TasA aggregates further interlink to form a gel-like network [1]. Thus, although we were unable to assess the molecular dynamics of TasA in our experiments, existing literature serves to support the theory that TasA can aggregate beyond the normal fibrillar morphology when exposed to a low extracellular pH.

In addition to TasA, EPS have the potential to aggregate in response to altered pH of the growth medium. Since EPS describes an entire class of at least 15 macromolecules on the *epsA-O* operon, rather than a single molecule, it is difficult to make conclusive calculations of the theoretical isoelectric point for these substances [56]. However, a study of combined EPS in *Bacillus megaterium* asserts that the experimental isoelectric point is pH 4.8, near which the EPS can be found in dense aggregates [58]. Thus, it is possible that

the collection of EPS in *B. subtilis* biofilms responds similarly to a low pH environment, despite some of the individual molecules having isoelectric points greater than one pH value away from the experimental pH.

Cell division defect theory

While the matrix aggregation theory is well supported by the literature, our microfluidics experiment points toward the presence of another property of these acidic colonies that may be driving the microcolony phenotype: chaining. When a bacterial cell divides by binary fission, a complex of enzymes and accessory proteins sometimes referred to as the divisome assembles along the cell wall to form the septum and drive the separation of the mother cell from the daughter cell. As evidenced by our microfluidics data, the cleavage of the cell wall upon division is significantly less efficient under acidic conditions than neutral, leading to the chaining phenotype we see. While several factors may be driving this chaining, we propose that the catalytic efficiency of the divisome is reduced because of altered enzyme and/or cell wall charges. The divisome-associated proteins identified in the literature are briefly summarized in Table 2 [40, 3, 5, 17]. Half of these proteins have isoelectric points near the pH of the acidic MM9 medium, introducing the potential for loss of charge and loss of proper function. It should be noted that the isoelectric point is a valuable metric for the entire protein, but more information about regional characteristics is needed to further understand the effects of pH on enzyme kinetics and protein-protein interactions.

However, since this complex is formed cooperatively with subunit recruitment by other subunits, a conformational change in one of the enzyme binding sites has the potential to disrupt the proper functioning of the entire complex. In addition, other non-divisome proteins are involved in division site selection and other divisome-related functions. For example, MinJ binds to the conserved C-terminal lipid-binding domain (LBD) on the divisome protein DivIVA and is involved in division-site selection under standard conditions. Experiments revealed that the truncation of the C-terminus of DivIVA prevents MinJ recruitment which results in increased chaining [2]. In addition, impaired DivIVA activity has been shown to inhibit swarming motility, in agreement with our findings [21]. Since this 60-amino acid LBD has a theoretical isoelectric point of 5.27, it is reasonable to expect a change in MinJ binding because of LBD conformation change if exposed to a low pH similar to that in this study. Although DivIVA is only one protein within the large divisome complex, it serves as an example of the potential effects that the disruption of one of these proteins could have on colony-scale morphology. Since many of the cell division proteins are localized within the cell, it is unknown whether the extracellular pH would directly affect protein-protein interactions in this way.

However, there is existing evidence of an association between a low pH growth environment and the suppression of murein (cell wall) hydrolases, possibly because of an altered cell wall ionic state [19, 57]. In addition, the presence of chaining in other bacterial species correlates with increased growth in the upward direction, like the apparent growth phenotype after 48+ hours of growth on acidic MM9 [38]. Thus, it is reasonable to expect

that the microcolony morphology in this experiment is at least partially influenced by the chaining of cells because of malfunctioning cell wall hydrolases.

Future directions

While the matrix aggregation theory has support from the existing literature, it is important that further experiments investigating this phenotype pursue the interactions occurring in the live biofilms we study. For example, using a sensitive aggregation fluorescent dye may enable imaging of protein aggregates and their localization in biofilms in time-lapse videos. In addition, these dyes may give insights into the relative amount of aggregation under both neutral and acidic conditions – adjusted for OD – when reading bulk fluorescence in plate reader experiments. Although we presently do not have access to biochemical assays and purification tools, this theory would greatly benefit from protein extraction tools and size-exclusion chromatography as well to differentiate between the normal fibrillar aggregation of TasA under neutral conditions and the aggregates we expect to find under acidic conditions.

To understand more about the cell division defect theory, next steps would involve some biochemistry and molecular biology experiments. Like others have done with TasA, it would be valuable to learn how the divisome protein complex responds to acidic media *in vitro*, in the absence of cells. If acidity alters the protein assembly and enzymatic efficiency in this system, then it is possible the same protein-protein interactions are occurring within the cells in our acidic MM9 media. Next, since the shape and ionic state of the cell wall are used to determine septum formation sites in a dividing cell, we would

want to assess whether the cell wall becomes less negative in an acidic environment by measuring membrane voltage under neutral and acidic conditions. Lastly, if we were able to tag the cell wall division proteins with fluorescent reporters, we could observe the subcellular localization of these proteins and determine if there is a defect in the assembly and/or localization of the divisome in response to an acidic environment.

Overall, since we aimed to move toward a more physiologically relevant experimental system with this project, there are many next steps that would allow us to expand the findings in this study. The following are some experimental design aspects that we would like to eventually include in our work: use of gas control to simulate the oxygen concentrations of the discrete gut compartments, coculture of several physiologically relevant microbial species throughout the environmental transitions, and use of organoid systems to account for the influence of host epithelia on these colony-scale morphologies [42, 26]. Each of these systems offers unique controls over environmental conditions that help us gain a deeper understanding of the microbial interactions in the dynamic gut microbiome environment.

CONCLUSION

This study aimed to investigate the ways in which *Bacillus subtilis* colonies change their morphologies in response to acidification of the environmental pH, as inspired by the human gut microbiome. We found that colonies grown on agar made from acidic media tend to grow in 'microcolonies' early in growth and have significantly reduced radial expansion during all stages of growth. Our experiments and literature searches support the pH-driven matrix protein aggregation and cell division defect theories. The majority of this work highlights colony morphologies in a static acidic-pH environment, but we hope to continue pursuing the question of how colonies respond to physiologically relevant pH transience.

TABLES & FIGURES

Table 1. Comparison of the common biofilm-inducing growth medium (Msgg) and the novel MM9 medium. Values identified with an asterisk vary slightly in the acidic variation of MM9.

Ion/Species in Solution	Msgg (mM)	Neutral MM9 (mM)
Glycerol	68.4	68.4
Glutamate	29.6	29.6
$\boldsymbol{Fe^{3+}}$	0.1	0.1
$\boldsymbol{Mn^{2+}}$	0.05	0.05
$\boldsymbol{Mg^{2+}}$	2	1
$\boldsymbol{Ca^{2+}}$	0.7	0.1
$\boldsymbol{K^{+}}$	811	22
$\boldsymbol{Zn^{2+}}$	9.98×10^{-4}	--
$\boldsymbol{Na^{+}}$	387	123*
$\boldsymbol{Cl^{-}}$	5.8	9.16
$\boldsymbol{SO_4^{2-}}$	1×10^{3}	1
$\boldsymbol{PO_4^{2-}}$	5×10^{2}	64.3

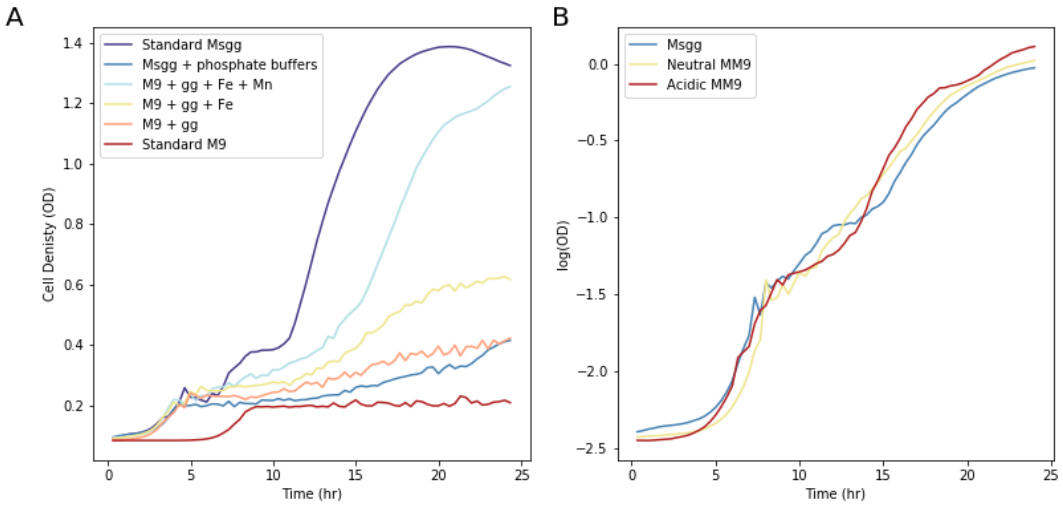

Figure 1. Testing the growth limitations of a titratable minimal medium. A) Lines represent the average values at each timepoint for 12 replicates. “+Fe” and “+Mn” = addition of Iron and Manganese salts in the concentrations found in Msgg. ”gg” = removal of glucose carbon source and replacement with glycerol and glutamate in the concentrations found in Msgg. B) Lines represent the average values at each timepoint for 24 replicates. Acidic MM9 is at a pH near 5.25, while neutral MM9 is pH 7.

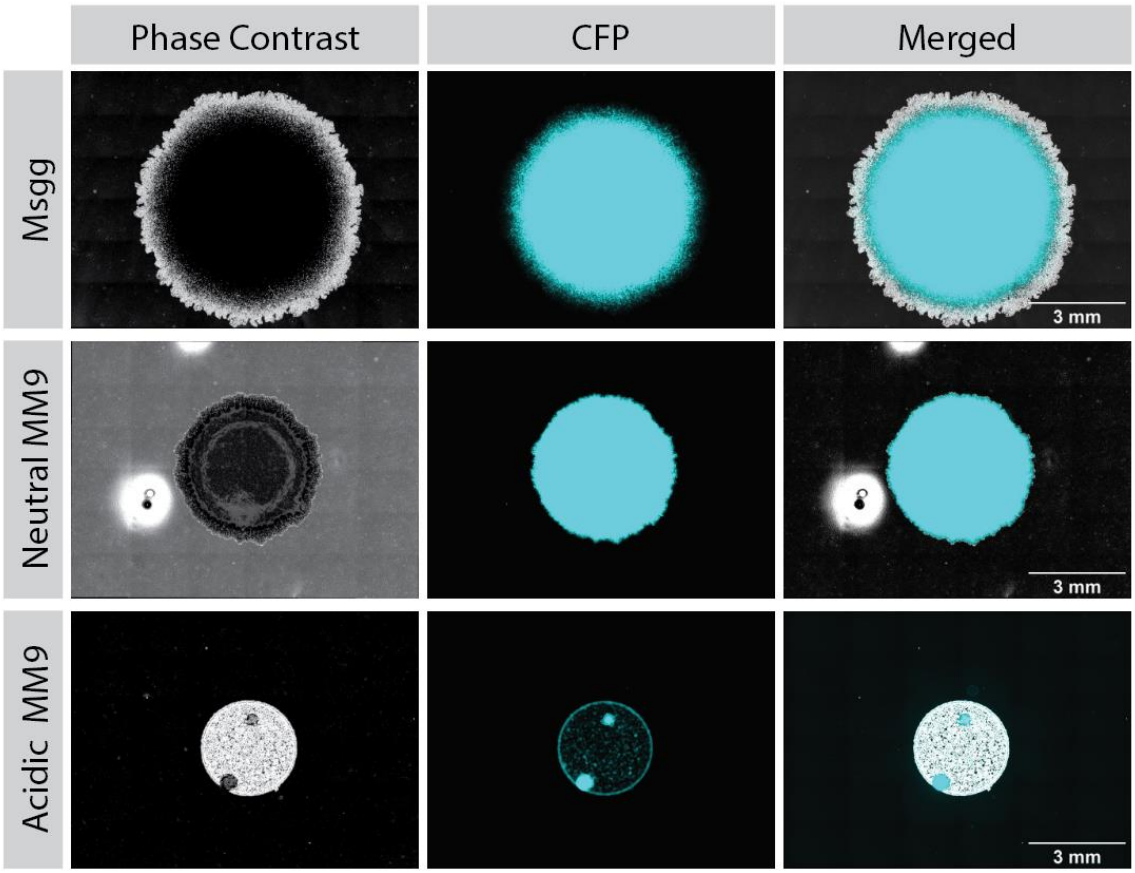

Figure 2. Identifying a novel growth phenotype on acidic MM9 agar. The Msgg image was taken at 25.67 hr. of growth, whereas the other two were taken at 33.33 hr. This is because the Msgg colony grew beyond the field of view at later timepoints. The CFP channel imaging ThT expression allows us to identify the locations of greatest cell density.

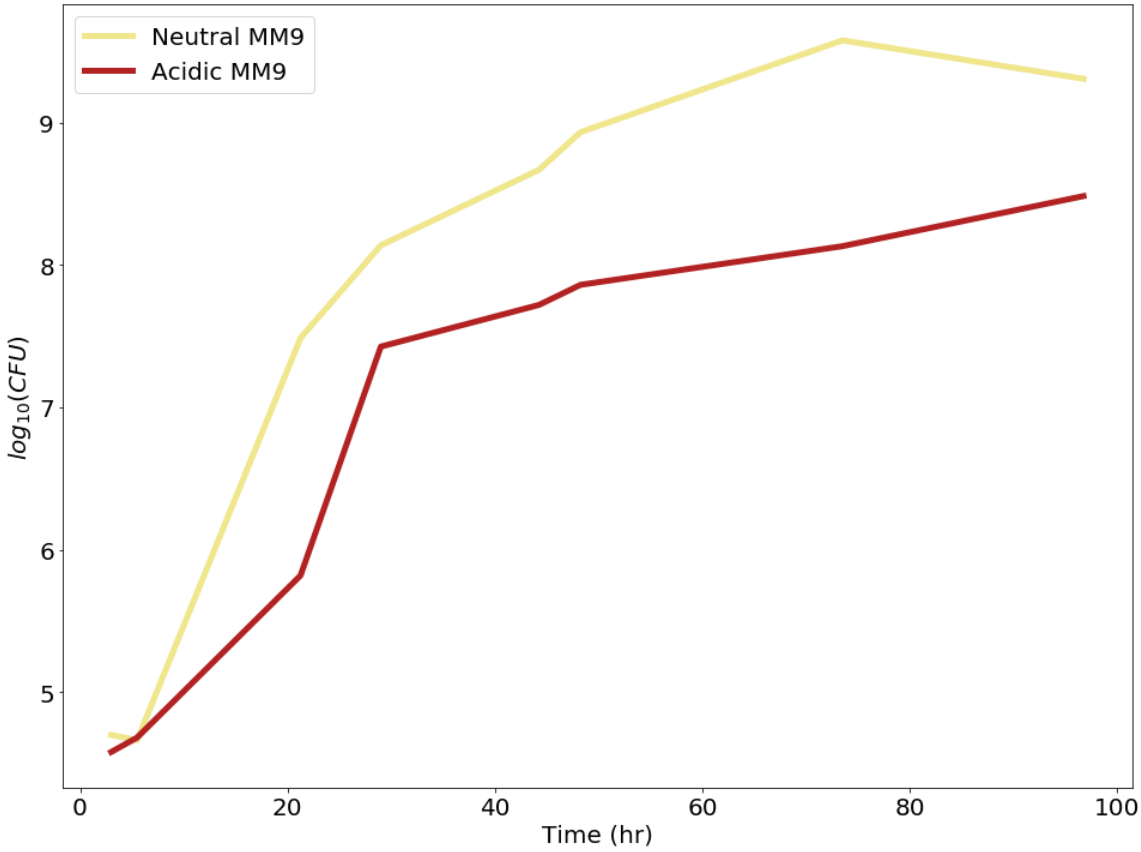

Figure 3. Assessing the growth differential between neutral and acidic colonies. Eight individual CFU counts were performed for both neutral and acidic colonies over the course of 96.75 hr., grown in parallel. Note: these CFU counts were not spaced equally apart due to overnight growth.

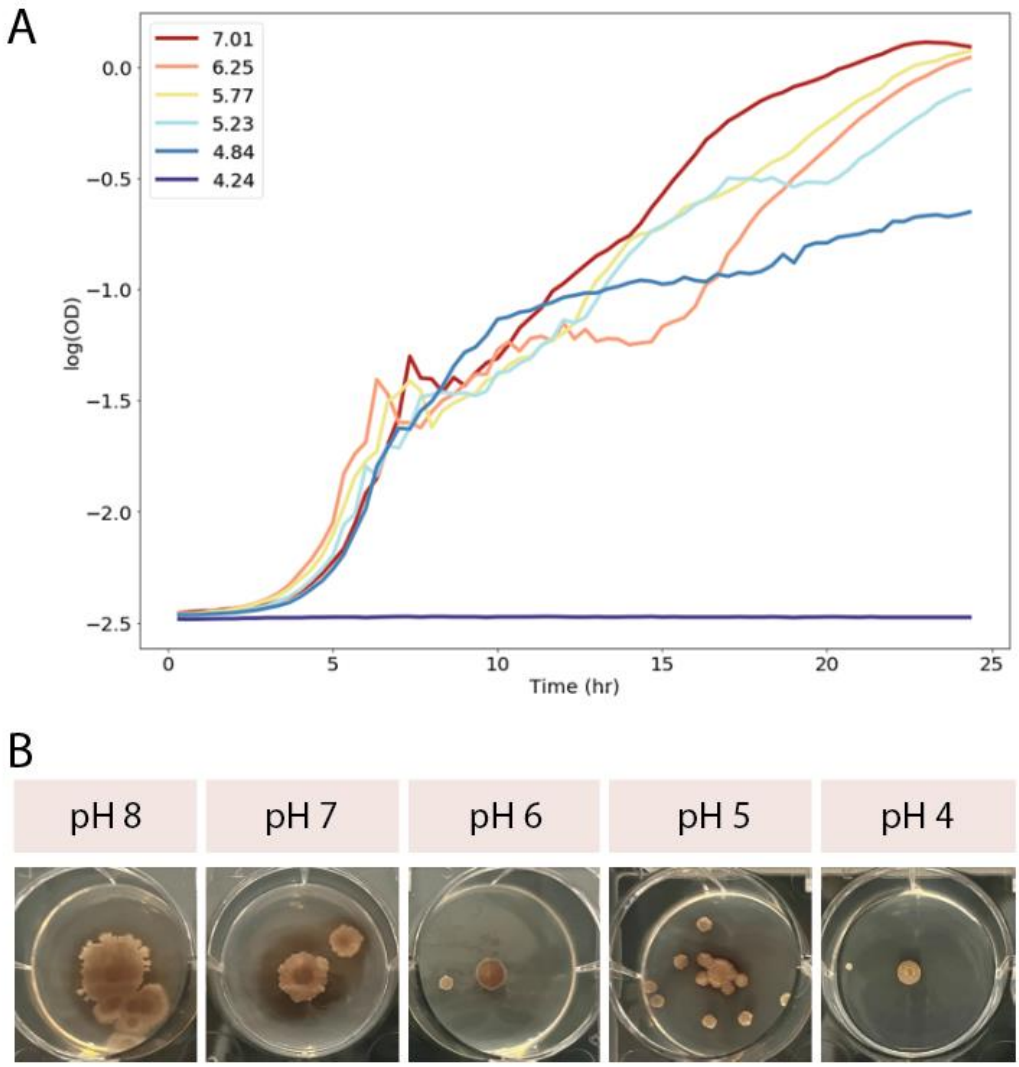

Figure 4. Determining growth and morphology responses to a pH gradient. A) Each line represents the average value for 12 replicates. Legend reflects pH values. All other experimental conditions were held equal between conditions. B) Hard substrate (1.5% agar) images of colonies grown for 3 days. From left to right: pH values of the agar are 8, 7, 6, 5, and 4, respectively. Satellite colonies are likely the result of moisture accumulation on the agar.

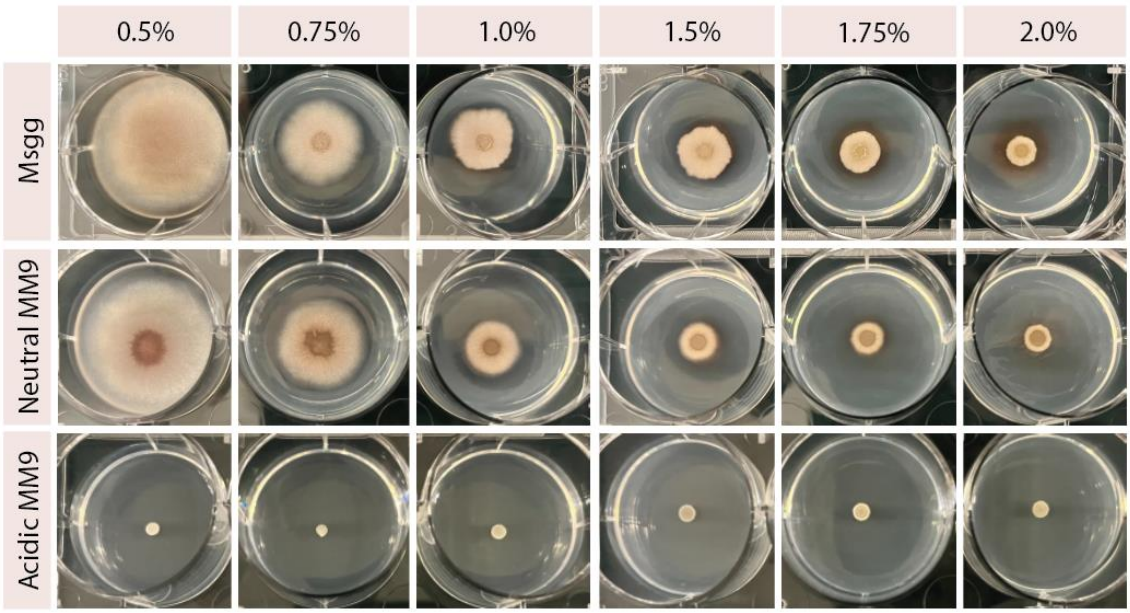

Figure 5. Agar percentage gradient reveals inability of acidic colonies to swarm. Photographed after 48 hours of growth. Each plate has the same agar percentage gradient from left to right: 0.5, 0.75, 1.0, 1.5, 1.75, and 2.0. Inability to swarm is determined based on minimal radial expansion on acidic MM9 even at low agar percentages.

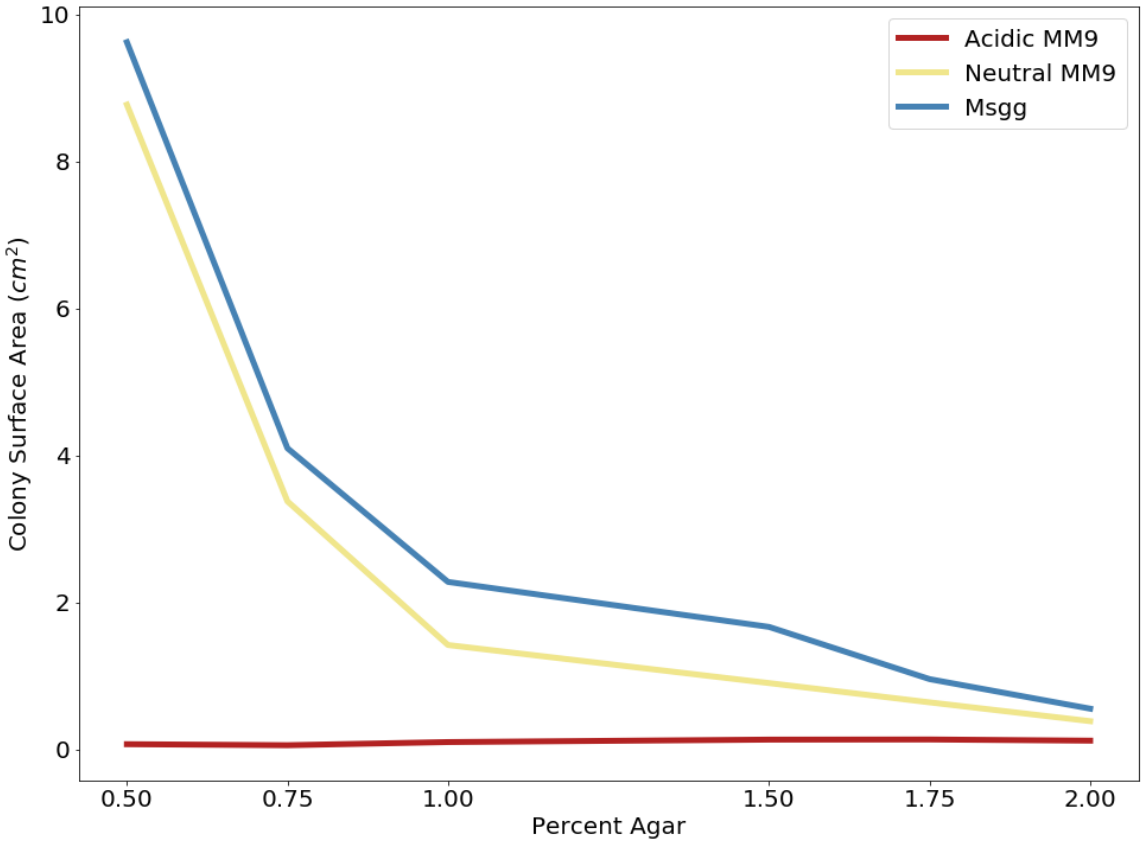

Figure 6. Colony surface area along an agar percentage gradient reflects a lack of swarming ability under acidic conditions. Calculations were made with ImageJ analysis of phase contrast images of the colonies pictured in Figure 5. Colony surface area is taken at 48 hr. of growth.

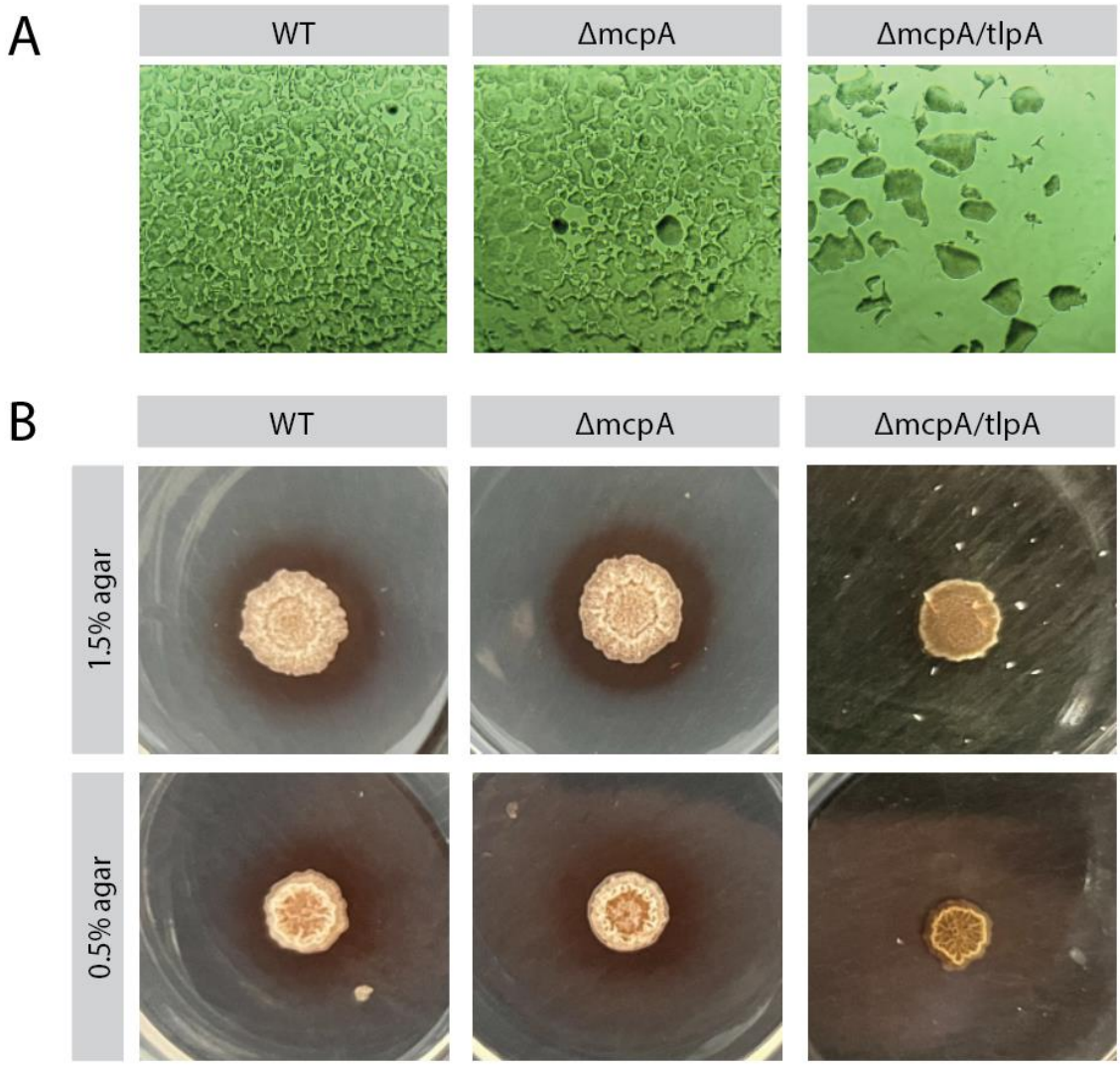

Figure 7. Observing the effect of gene knockouts on acidic MM9 colony morphology. All images are of colonies grown on acidic MM9 agar. A) Brightfield images taken at 10X magnification after 18 hours of growth. Growth appears clustered in all three strains. B) No-magnification images of colonies after one week of growth (maximum growth) on 1.5% and 0.5% agar, respectively. While there are some morphological differences between the three strains, all colonies have similarly minimal radial expansion, suggesting the phenotype is unrelated to the deleted chemotaxis genes.

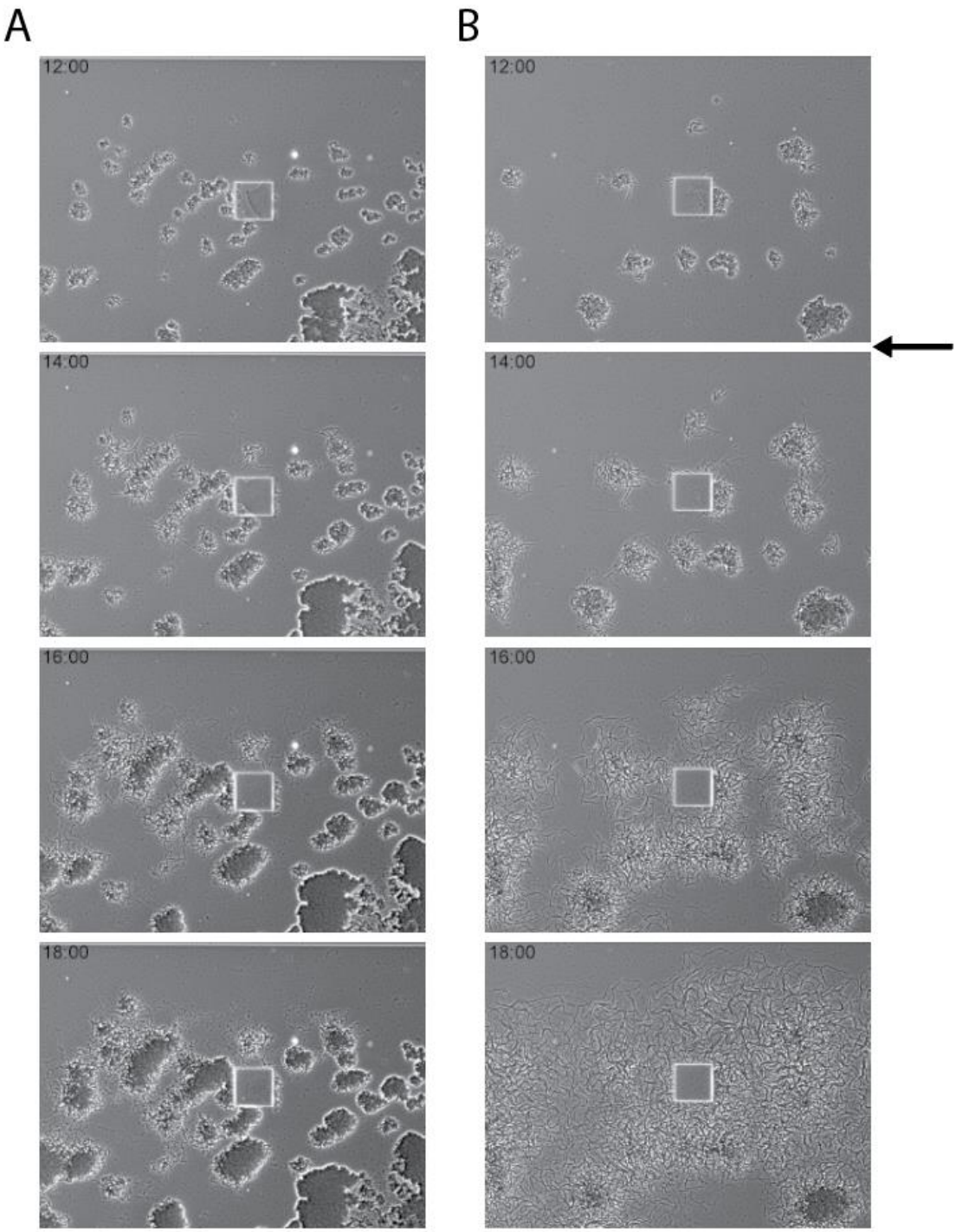

Figure 8. Observing colony responses to a transition from neutral to acidic MM9 in a microfluidics device. All images taken at 4X magnification. A) Neutral MM9 control. B) Arrow indicates that the media was switched to acidic MM9 after 12 hr. of growth in neutral MM9.

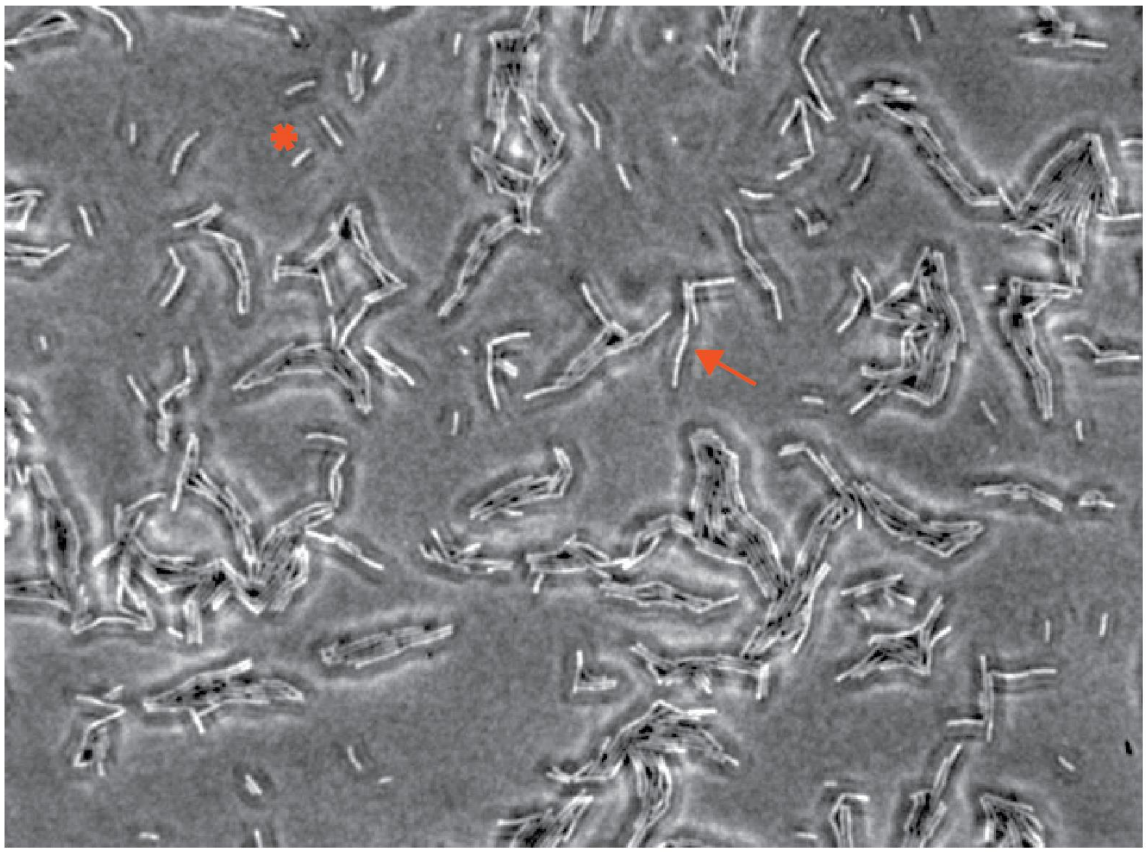

Figure 9. Identification of acid-induced chaining on inverted agar pad. Imaged at 40X magnification. A non-chaining single cell is denoted by * for reference. The arrow points to an example of a growing chain.

Table 2. B. subtilis divisome proteins. Subunits are recruited in roughly the order displayed. Grey boxes denote an isoelectric point within 1 pH unit of the acidic MM9 media. This list has been compiled using existing literature but should not be used as a comprehensive summary of cell division-related proteins.

Protein name(s)	Function	Localization during division	Theoretical isoelectric point
FtsZ	Cell division initiation; septum formation via Z-ring formation.	Septum/ membrane	4.81
FtsA	Membrane anchor for FtsZ.	Septum/ membrane	5.09
SepF	Recruitment of FtsZ to cell membrane and determining thickness of septal cell wall.	Septum/ membrane	4.86
ZapA	Positively modulates Z-ring formation and stability.	Cytoplasm	7.17
EzrA	Negatively modulates Z-ring formation via inhibition of FtsZ.	Membrane	4.76
GpsB	Adaptor protein for multiple cell wall enzymes.	Cytoplasm	5.63
FtsL	DivIB-FtsL-DivIC complex recruits FtsW and Pbp2B.	Membrane	10.08
DivIB	DivIB-FtsL-DivIC complex recruits FtsW and Pbp2B.	Membrane	9.24
DivIC	DivIB-FtsL-DivIC complex recruits FtsW and Pbp2B. Stabilizes ftsL against cleavage.	Membrane	9.97
FtsW	Principal divisome peptidoglycan glycosyltransferase. Septal cell wall synthesis.	Membrane, co-localized with FtsZ	9.72
Pbp2B	Works with FtsW in septal cell wall synthesis.	Membrane	9.23
DivIVA	Curvature-sensitive septum placement. Recruits other cytoplasmic proteins.	Dynamic, cytoplasm	4.85
MinC	Inhibits reinitiation of divisome.	Membrane	6.26
MinD	Inhibits reinitiation of divisome.	Membrane	4.98

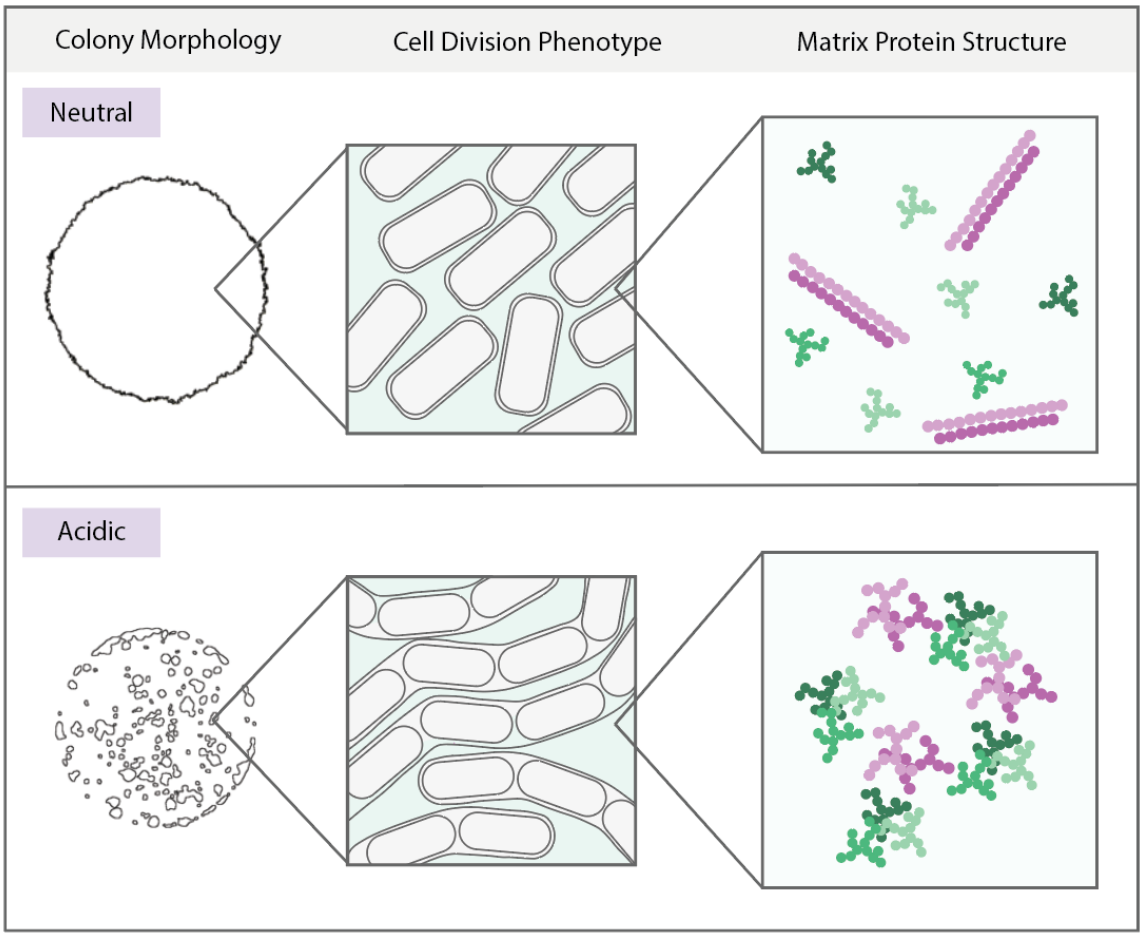

Figure 10. *Proposed explanation for growth phenotype under acidic conditions*. Colony outlines were developed from ImageJ ROIs of real colony growth movies. The remainder of the cartoon serves as an illustration of the cell division defect and matrix aggregation theories.

BIBLIOGRAPHY

1. Azulay, D. N., Ghrayeb, M., Ktorza, I. B., Nir, I., Nasser, R., Harel, Y. S., & Chai, L. (2020). Colloidal-like aggregation of a functional amyloid protein. *Physical Chemistry Chemical Physics*, *22*(40), 23286–23294. https://doi.org/10.1039/D0CP03265D

2. Baarle, S. van, Celik, I. N., Kaval, K. G., Bramkamp, M., Hamoen, L. W., & Halbedel, S. (2012). Protein-Protein Interaction Domains of Bacillus subtilis DivIVA. *Journal of Bacteriology*. https://journals.asm.org/doi/abs/10lecler.1128/JB.02171-12

3. Bach, J., Albrecht, N., & Bramkamp, M. (2014). Imaging DivIVA dynamics using photo-convertible and activatable fluorophores in Bacillus subtilis. *Frontiers in Microbiology*, *5*. https://www.frontiersin.org/article/10.3389/fmicb.2014.00059

4. Beauregard, P. B., Chai, Y., Vlamakis, H., Losick, R., & Kolter, R. (2013). *Bacillus subtilis* biofilm induction by plant polysaccharides. *Proceedings of the National Academy of Sciences*, *110*(17). https://doi.org/10.1073/pnas.1218984110

5. Bhambhani, A., Iadicicco, I., Lee, J., Ahmed, S., Belfatto, M., Held, D., Marconi, A., Parks, A., Stewart, C. R., Margolin, W., Levin, P. A., & Haeusser, D. P. (2020). Bacteriophage SP01 Gene Product 56 Inhibits Bacillus subtilis Cell Division by Interacting with FtsL and Disrupting Pbp2B and FtsW Recruitment. *Journal of Bacteriology*, *203*(2). https://doi.org/10.1128/JB.00463-20

6. Bloemendaal, M., Szopinska-Tokov, J., Belzer, C., Boverhoff, D., Papalini, S., Michels, F., van Hemert, S., Arias Vasquez, A., & Aarts, E. (2021). Probiotics-induced changes in gut microbial composition and its effects on cognitive performance after stress: exploratory analyses. *Translational Psychiatry*, *11*(1), 1–11. https://doi.org/10.1038/s41398-021-01404-9

7. Branda, S. S., Chu, F., Kearns, D. B., Losick, R., & Kolter, R. (2006). A major protein component of the Bacillus subtilis biofilm matrix. *Molecular Microbiology*, *59*(4), 1229–1238. https://doi.org/10.1111/j.1365-2958.2005.05020.x

8. Bruno, G., Zaccari, P., Rocco, G., Scalese, G., Panetta, C., Porowska, B., Pontone, S., & Severi, C. (2019). Proton pump inhibitors and dysbiosis: Current knowledge and aspects to be clarified. *World Journal of Gastroenterology*, *25*(22), 2706–2719. https://doi.org/10.3748/wjg.v25.i22.2706

9. Bull, M. J., & Plummer, N. T. (2014). Part 1: The Human Gut Microbiome in Health and Disease. *Integrative Medicine: A Clinician's Journal*, *13*(6), 17–22. https://www.ncbi.nlm.nih.gov/pmc/articles/PMC4566439/

10. *Coblis — Color Blindness Simulator – Colblindor*. (n.d.). Retrieved January 3, 2022, from https://www.color-blindness.com/coblis-color-blindness-simulator/

11. Cold Spring Harbor Protocols. M9 recipe. *Cold Spring Harb. Protoc.* **2006**, *2006*.

12. Colom, J., Freitas, D., Simon, A., Brodkorb, A., Buckley, M., Deaton, J., & Winger, A. M. (2021). Presence and Germination of the Probiotic Bacillus subtilis DE111® in the Human Small Intestinal Tract: A Randomized, Crossover, Double-Blind, and Placebo-Controlled Study. *Frontiers in Microbiology*, *12*. https://www.frontiersin.org/article/10.3389/fmicb.2021.715863

13. Costerton, J. W., Stewart, P. S., & Greenberg, E. P. (1999). Bacterial Biofilms: A Common Cause of Persistent Infections. *Science*. https://doi.org/10.1126/science.284.5418.1318

14. Derrien, M., & Vlieg, J. E. T. van H. (2015). Fate, activity, and impact of ingested bacteria within the human gut microbiota. *Trends in Microbiology*, *23*(6), 354–366. https://doi.org/10.1016/j.tim.2015.03.002

15. Diehl, A., Roske, Y., Ball, L., Chowdhury, A., Hiller, M., Molière, N., Kramer, R., Stöppler, D., Worth, C. L., Schlegel, B., Leidert, M., Cremer, N., Erdmann, N., Lopez, D., Stephanowitz, H., Krause, E., Rossum, B.-J. van, Schmieder, P., Heinemann, U., … Oschkinat, H. (2018). Structural changes of TasA in biofilm formation of Bacillus subtilis. *Proceedings of the National Academy of Sciences*, *115*(13), 3237–3242. https://doi.org/10.1073/pnas.1718102115

16. Fallingborg, J. (1999). Intraluminal pH of the human gastrointestinal tract. *Danish Medical Bulletin*, *46*(3), 183–196.

17. Gamba, P., Veening, J.-W., Saunders, N. J., Hamoen, L. W., & Daniel, R. A. (2009). Two-Step Assembly Dynamics of the *Bacillus subtilis* Divisome. *Journal of Bacteriology*, *191*(13), 4186–4194. https://doi.org/10.1128/JB.01758-08

18. Ghrayeb, M., Hayet, S., Lester-Zer, N., Levi-Kalisman, Y., & Chai, L. (2021). Fibrilar Polymorphism of the Bacterial Extracellular Matrix Protein TasA. *Microorganisms*, *9*(3), 529. https://doi.org/10.3390/microorganisms9030529

19. Goodell, E. W., Lopez, R., & Tomasz, A. (1976). Suppression of lytic effect of beta lactams on Escherichia coli and other bacteria. *Proceedings of the National Academy of Sciences*, *73*(9), 3293–3297. https://doi.org/10.1073/pnas.73.9.3293

20. Guan, N., & Liu, L. (2020). Microbial response to acid stress: mechanisms and applications. *Applied Microbiology and Biotechnology*, *104*(1), 51–65. https://doi.org/10.1007/s00253-019-10226-1

21. Hammond, L. R., White, M. L., & Eswara, P. J. (2019). ¡vIVA la DivIVA! *Journal of Bacteriology*. https://doi.org/10.1128/JB.00245-19

22. Hamouche, L., Laalami, S., Daerr, A., Song, S., Holland, I. B., Séror, S. J., Hamze, K., & Putzer, H. (2017). Bacillus subtilis Swarmer Cells Lead the Swarm, Multiply, and Generate a Trail of Quiescent Descendants. *MBio*. https://doi.org/10.1128/mBio.02102-16

23. Hasan, N., & Yang, H. (2019). Factors affecting the composition of the gut microbiota, and its modulation. *PeerJ*, *7*, e7502. https://doi.org/10.7717/peerj.7502

24. Hernández-Jiménez, E., Del Campo, R., Toledano, V., Vallejo-Cremades, M. T., Muñoz, A., Largo, C., Arnalich, F., García-Rio, F., Cubillos-Zapata, C., & López-Collazo, E. (2013). Biofilm vs. planktonic bacterial mode of growth: which do human macrophages prefer? *Biochemical and Biophysical Research Communications*, *441*(4), 947–952. https://doi.org/10.1016/j.bbrc.2013.11.012

25. Ilinskaya, O. N., Ulyanova, V. V., Yarullina, D. R., & Gataullin, I. G. (2017). Secretome of Intestinal Bacilli: A Natural Guard against Pathologies. *Frontiers in Microbiology*, *8*. https://www.frontiersin.org/article/10.3389/fmicb.2017.01666

26. Jalili-Firoozinezhad, S., Gazzaniga, F. S., Calamari, E. L., Camacho, D. M., Fadel, C. W., Bein, A., Swenor, B., Nestor, B., Cronce, M. J., Tovaglieri, A., Levy, O., Gregory, K. E., Breault, D. T., Cabral, J. M. S., Kasper, D. L., Novak, R., & Ingber, D. E. (2019). A complex human gut microbiome cultured in an anaerobic intestine-on-a-chip. *Nature Biomedical Engineering*, *3*(7), 520–531. https://doi.org/10.1038/s41551-019-0397-0

27. Jiang, Q., He, X., Zou, Y., Ding, Y., Li, H., & Chen, H. (2018). Altered gut microbiome promotes proteinuria in mice induced by Adriamycin. *AMB Express*, *8*(1), 31. https://doi.org/10.1186/s13568-018-0558-7

28. Kho, Z. Y., & Lal, S. K. (2018). The Human Gut Microbiome – A Potential Controller of Wellness and Disease. *Frontiers in Microbiology*, *9*. https://www.frontiersin.org/article/10.3389/fmicb.2018.01835

29. Kong, X., Liu, J., Liu, K., Koh, M., Tian, R., Hobbie, C., Fong, M., Chen, Q., Zhao, M., Budjan, C., & Kong, J. (2020). Altered Autonomic Functions and Gut Microbiome in Individuals with Autism Spectrum Disorder (ASD): Implications for Assisting ASD Screening and Diagnosis. *Journal of Autism and Developmental Disorders*. https://doi.org/10.1007/s10803-020-04524-1

30. Krulwich, T. A., Agus, R., Schneier, M., & Guffanti, A. A. (1985). Buffering capacity of bacilli that grow at different pH ranges. *Journal of Bacteriology*, *162*(2), 768–772. https://www.ncbi.nlm.nih.gov/pmc/articles/PMC218917/

31. Lagier, J.-C., Dubourg, G., Million, M., Cadoret, F., Bilen, M., Fenollar, F., Levasseur, A., Rolain, J.-M., Fournier, P.-E., & Raoult, D. (2018). Culturing the human microbiota and culturomics. *Nature Reviews Microbiology*, *16*(9), 540–550. https://doi.org/10.1038/s41579-018-0041-0

32. Leclercq, S., Matamoros, S., Cani, P. D., Neyrinck, A. M., Jamar, F., Stärkel, P., Windey, K., Tremaroli, V., Bäckhed, F., Verbeke, K., de Timary, P., & Delzenne, N. M. (2014). Intestinal permeability, gut-bacterial dysbiosis, and behavioral markers of alcohol-dependence severity. *Proceedings of the National Academy of Sciences*, *111*(42), E4485–E4493. https://doi.org/10.1073/pnas.1415174111

33. Ley, R. E., Hamady, M., Lozupone, C., Turnbaugh, P. J., Ramey, R. R., Bircher, J. S., Schlegel, M. L., Tucker, T. A., Schrenzel, M. D., Knight, R., & Gordon, J. I. (2008). Evolution of mammals and their gut microbes. *Science (New York, N.Y.)*, *320*(5883), 1647–1651. https://doi.org/10.1126/science.1155725

34. Lin, L., Zheng, L. J., & Zhang, L. J. (2018). Neuroinflammation, Gut Microbiome, and Alzheimer's Disease. *Molecular Neurobiology*, *55*(11), 8243–8250. https://doi.org/10.1007/s12035-018-0983-2

35. Martinez-Guryn, K., Leone, V., & Chang, E. B. (2019). Regional Diversity of the Gastrointestinal Microbiome. *Cell Host & Microbe*, *26*(3), 314–324. https://doi.org/10.1016/j.chom.2019.08.011

36. Marvasi, M., Visscher, P. T., & Casillas Martinez, L. (2010). Exopolymeric substances (EPS) from Bacillus subtilis: polymers and genes encoding their synthesis. *FEMS Microbiology Letters*, *313*(1), 1–9. https://doi.org/10.1111/j.1574-6968.2010.02085.x

37. Maseda, D., Zackular, J. P., Trindade, B., Kirk, L., Roxas, J. L., Rogers, L. M., Washington, M. K., Du, L., Koyama, T., Viswanathan, V. K., Vedantam, G., Schloss, P. D., Crofford, L. J., Skaar, E. P., & Aronoff, D. M. (2019). Nonsteroidal Anti-inflammatory Drugs Alter the Microbiota and Exacerbate Clostridium difficile Colitis while Dysregulating the Inflammatory Response. *MBio*, *10*(1), e02282-18. https://doi.org/10.1128/mBio.02282-18

38. Matysik, A., Ho, F. K., Ler Tan, A. Q., Vajjala, A., & Kline, K. A. (2020). Cellular chaining influences biofilm formation and structure in group A Streptococcus. *Biofilm*, *2*, 100013. https://doi.org/10.1016/j.bioflm.2019.100013

39. Maurer, J. M., Schellekens, R. C. A., van Rieke, H. M., Wanke, C., Iordanov, V., Stellaard, F., Wutzke, K. D., Dijkstra, G., van der Zee, M., Woerdenbag, H. J., Frijlink, H. W., & Kosterink, J. G. W. (2015). Gastrointestinal pH and Transit Time Profiling in Healthy Volunteers Using the IntelliCap System Confirms Ileo-Colonic Release of ColoPulse Tablets. *PloS One*, *10*(7), e0129076. https://doi.org/10.1371/journal.pone.0129076

40. Pedreira, T., Elfmann, C., & Stülke, J. (2021). The current state of *Subti* Wiki, the database for the model organism *Bacillus subtilis*. *Nucleic Acids Research*, gkab943. https://doi.org/10.1093/nar/gkab943

41. Peng, J., Xiao, X., Hu, M., & Zhang, X. (2018). Interaction between gut microbiome and cardiovascular disease. *Life Sciences*, *214*, 153–157. https://doi.org/10.1016/j.lfs.2018.10.063

42. Rahmani, S., Breyner, N. M., Su, H.-M., Verdu, E. F., & Didar, T. F. (2019). Intestinal organoids: A new paradigm for engineering intestinal epithelium in vitro. *Biomaterials*, *194*, 195–214. https://doi.org/10.1016/j.biomaterials.2018.12.006

43. Ramirez, J., Guarner, F., Bustos Fernandez, L., Maruy, A., Sdepanian, V. L., & Cohen, H. (2020). Antibiotics as Major Disruptors of Gut Microbiota. *Frontiers in Cellular and Infection Microbiology*, *10*. https://www.frontiersin.org/article/10.3389/fcimb.2020.572912

44. Rinninella, E., Raoul, P., Cintoni, M., Franceschi, F., Miggiano, G. A. D., Gasbarrini, A., & Mele, M. C. (2019). What is the Healthy Gut Microbiota Composition? A Changing Ecosystem across Age, Environment, Diet, and Diseases. *Microorganisms*, *7*(1), 14. https://doi.org/10.3390/microorganisms7010014

45. Robitaille, S., Trus, E., & Ross, B. D. (2021). Bacterial Defense against the Type VI Secretion System. *Trends in Microbiology*, *29*(3), 187–190. https://doi.org/10.1016/j.tim.2020.09.001

46. Rosillo-Lopez, M., & Salzmann, C. G. (2018). Highly efficient heavy-metal extraction from water with carboxylated graphene nanoflakes. *RSC Advances*, *8*(20), 11043–11050. https://doi.org/10.1039/C8RA00823J

47. Roychowdhury, S., Selvakumar, P., & Cresci, G. (2018). The Role of the Gut Microbiome in Nonalcoholic Fatty Liver Disease. *Medical Sciences*, *6*(2), 47. https://doi.org/10.3390/medsci6020047

48. Schneider, C. A., Rasband, W. S., & Eliceiri, K. W. (2012). NIH Image to ImageJ: 25 years of image analysis. *Nature Methods*, *9*(7), 671–675. doi:10.1038/nmeth.2089

49. Shao, L., Ling, Z., Chen, D., Liu, Y., Yang, F., & Li, L. (2018). Disorganized Gut Microbiome Contributed to Liver Cirrhosis Progression: A Meta-Omics-Based Study. *Frontiers in Microbiology*, *9*, 3166. https://doi.org/10.3389/fmicb.2018.03166

50. Shemesh, M., & Chai, Y. (2013). A Combination of Glycerol and Manganese Promotes Biofilm Formation in Bacillus subtilis via Histidine Kinase KinD Signaling. *Journal of Bacteriology*, *195*(12), 2747–2754. https://doi.org/10.1128/JB.00028-13

51. *Spizizen's salts - 2010.igem.org*. (n.d.). Retrieved January 3, 2022, from http://2010.igem.org/Spizizen's_salts

52. Tam, N. K. M., Uyen, N. Q., Hong, H. A., Duc, L. H., Hoa, T. T., Serra, C. R., Henriques, A. O., & Cutting, S. M. (2006). The Intestinal Life Cycle of Bacillus subtilis and Close Relatives. *Journal of Bacteriology*, *188*(7), 2692–2700. https://doi.org/10.1128/JB.188.7.2692-2700.2006

53. Tohidifar, P., Plutz, M. J., Ordal, G. W., & Rao, C. V. (n.d.). The Mechanism of Bidirectional pH Taxis in Bacillus subtilis. *Journal of Bacteriology*, *202*(4), e00491-19. https://doi.org/10.1128/JB.00491-19

54. Turnbaugh, P. J., Ley, R. E., Hamady, M., Fraser-Liggett, C., Knight, R., & Gordon, J. I. (2007). The human microbiome project: exploring the microbial part of ourselves in a changing world. *Nature*, *449*(7164), 804–810. https://doi.org/10.1038/nature06244

55. Ursell, L. K., Metcalf, J. L., Parfrey, L. W., & Knight, R. (2012). Defining the Human Microbiome. *Nutrition Reviews*, *70*(Suppl 1), S38–S44. https://doi.org/10.1111/j.1753-4887.2012.00493.x

56. Vlamakis, H., Chai, Y., Beauregard, P., Losick, R., & Kolter, R. (2013). Sticking together: building a biofilm the Bacillus subtilis way. *Nature Reviews. Microbiology*, *11*(3), 157–168. https://doi.org/10.1038/nrmicro2960

57. Vollmer, W., Joris, B., Charlier, P., & Foster, S. (2008). Bacterial peptidoglycan (murein) hydrolases. *FEMS Microbiology Reviews*, *32*(2), 259–286. https://doi.org/10.1111/j.1574-6976.2007.00099.x

58. Wang, L.-L., Wang, L.-F., Ren, X.-M., Ye, X.-D., Li, W.-W., Yuan, S.-J., Sun, M., Sheng, G.-P., Yu, H.-Q., & Wang, X.-K. (2012). pH dependence of structure and surface properties of microbial EPS. *Environmental Science & Technology*, *46*(2), 737–744. https://doi.org/10.1021/es203540w

59. Yang, Y., Tian, J., & Yang, B. (2018). Targeting gut microbiome: A novel and potential therapy for autism. *Life Sciences*, *194*, 111–119. https://doi.org/10.1016/j.lfs.2017.12.027

60. Yekani, M., Baghi, H. B., Naghili, B., Vahed, S. Z., Sóki, J., & Memar, M. Y. (2020). To resist and persist: Important factors in the pathogenesis of Bacteroides fragilis. *Microbial Pathogenesis*, *149*, 104506. https://doi.org/10.1016/j.micpath.2020.104506

61. Yonezawa, H., Osaki, T., & Kamiya, S. (2015). Biofilm Formation by Helicobacter pylori and Its Involvement for Antibiotic Resistance. *BioMed Research International*, *2015*, 914791. https://doi.org/10.1155/2015/914791

62. Zhang, C., Derrien, M., Levenez, F., Brazeilles, R., Ballal, S. A., Kim, J., Degivry, M.-C., Quéré, G., Garault, P., van Hylckama Vlieg, J. E. T., Garrett, W. S., Doré, J., & Veiga, P. (2016). Ecological robustness of the gut microbiota in response to ingestion of transient food-borne microbes. *The ISME Journal*, *10*(9), 2235–2245. https://doi.org/10.1038/ismej.2016.13